

Chapter

Mechanistic Dissection of Macular Degeneration Using the Phosphorylation Interactome

Weilue He, Srinivas R. Sripathi, Madu Joshua, Ruonan Zhang, Fabunmi Tosin, Patrick Ambrose, Diana R. Gutsaeva and Wan Jin Jahng

Abstract

In the current study, we suggest that phosphorylation reactions of specific proteins in mitochondria and the nucleus are a key step in the progression of age-related macular degeneration (AMD). To determine the molecular mechanism of AMD, we examined proteomic changes under oxidative stress to establish the protein interaction map using *in vitro* and *in vivo* models that mimic the complex and progressive characteristics of AMD. We postulated that apoptosis can be initiated by phosphorylation reactions under chronic oxidative stress in a region-specific and tissue-specific manner. The analysis of AMD interactome and oxidative biomarker network demonstrated that the presence of tissue- and region-dependent post-translational mechanisms may contribute toward AMD progression through the mitochondrial-nuclear communication. The AMD interactome suggests that new therapeutic targets, including prohibitin, erythropoietin, vitronectin, crystalline, nitric oxide synthase, ubiquitin, and complement inhibition may exist as a proteome network. Further, immunocytochemistry demonstrated that mitochondria could enter the nucleus in the retinal pigment epithelium (RPE) under oxidative stress. The current interactome map implies that a positive correlation may exist between oxidative stress-mediated phosphorylation and AMD progression. The unbiased proteome network provides a basis for understanding oxidative stress-induced mitochondrial dysfunction in AMD and exploring effective therapeutic approaches to treat age-related neurodegeneration.

Keywords: protein interactome, mitochondria, phosphoproteomics, prohibitin, retrograde signaling, AMD target

1. Introduction

Age-related macular degeneration (AMD) is the leading cause of legal blindness in developed countries [1, 2]. Although the vision loss directly results from dysfunction and cell death of photoreceptors in the central retina, it has been demonstrated that the early stage of AMD involves the pathological changes in retinal pigment epithelium (RPE), the cell layer that plays pivotal roles in supporting photoreceptors. Due to the inevitable roles of RPE in supporting retinal function, it is critical to understand the physiological and pathological events in the RPE to prevent the development of AMD.

AMD symptoms include RPE atrophy, drusen accumulation, pigmentary changes, and choroidal neovascularization [1, 2]. Progressive cell death of post-mitotic RPE can lead to rod and cone apoptosis, resulting in AMD eventually. As AMD is a complex and multifactorial disease, AMD mechanisms could be discussed under environmental and genetic factors, including oxidative stress (smoking, light exposure, and hypoxia), RPE dysfunction (retinoid recycling, phagocytosis, aging, and apoptosis), accumulation of visual cycle waste, chronic inflammation (involving CFH, CFB/C2, C3, CF1, C5, and C9), drusen formation (lipid metabolism involving APOE, LIPC, and CETP), geographic atrophy, and choroidal neovascularization (VEGF signaling) [3–8].

Recently, mitochondrial alterations have drawn great deal of attention in understanding AMD [3]. Mitochondrion is the main cell compartment for cell respiration and cell signaling. Many studies have shown that RPE mitochondria undergo severe structural and functional changes during aging and AMD [3, 4]. The mitochondrial dysfunction causes the excessive generation and leaking of reactive oxidative species (ROS) from the respiration chain and RPE is one of the most susceptible cells to ROS. RPE is also responsible for phagocytosis of rod outer segments, where polyunsaturated fatty acids abound. Phagocytosis and oxidation of unsaturated fatty acids generate additional ROS. Further, RPE cells are exposed to chronic oxidative stress, including constant exposure to intense light and oxidants from mitochondria due to high levels of oxygen demand and consumption. The increased oxidative stress in RPE may in turn deteriorates mitochondria and causes RPE cell death. Our data suggested that mitochondrial morphology and functional integrity are closely related to apoptosis and cellular aging [9–11]. Insufficient bioenergetic processes may lead to drusen accumulation. A number of apoptotic regulators reside in mitochondria and various retrograde signaling mechanisms are also dependent on mitochondria.

Oxidative stress facilitates the formation of toxic lipids and protein peroxidation, resulting in drusen deposition. There are excessive generation and leaking of oxidants from the respiratory chain under oxidative stress. This explains why AMD is associated with the accumulation of advanced lipid peroxidation end products, leading to apoptosis of photoreceptors and RPE cells. In addition, phosphorylation of crystalline and vimentin may participate in the pathogenesis of AMD by forming soft drusen with longer chain of phosphatidylcholine and cholesteryl esters. With aging, lipids and cholesterol accumulate underneath the RPE and contribute toward drusen formation. The excessive drusen deposition may damage the RPE and lead to degeneration of collagen or elastin in Bruch's membrane, the outer retina, and the choroid vasculature.

We have studied the mechanism of RPE cell death under various stress conditions [9–20]. Our data demonstrated that mitochondrial morphological changes and mitochondrial-nuclear shuttling of prohibitin are significant responses in the RPE under oxidative stress [9, 10, 18]. Herein, we discuss AMD mechanisms based on four distinctive subnetworks of protein interactome, including complement activation, transcriptional regulation, mitochondrial signaling, and apoptosis. We propose that altered retrograde mitochondrial-nuclear crosstalk may initiate the pathological reactions observed in aging and oxidative stress-mediated RPE cell death that can contribute to the pathogenesis of AMD.

2. Materials and methods

2.1 *In vivo* experimental design

All the animal procedures were performed in compliance with the Association for Research in Vision and Ophthalmology Statement for the humane use of laboratory

animals. Human *postmortem* donor eye tissues were used following the tenets of the Declaration of Helsinki. Diabetic retinopathy (DR) human retinal tissues (n = 9, biological triplicate × technical triplicate) were obtained from the Georgia Eye Bank (Atlanta, GA). AMD retina (8 mm macular and peripheral punches), RPE (8 mm central and peripheral punches), and age-matched control eyes (n = 9, biological triplicate × technical triplicate) were provided by the Lions Eye Bank (Moran Eye Center, University of Utah). Phosphoproteomes of macula (I), peripheral retina (II), central RPE (III), and peripheral RPE (IV) were compared to age-matched control donor eyes to determine region-specific, senescence-associated molecular mechanisms during AMD progression. Phosphoproteins were enriched by charge-based spin column chromatography and resolved by 2D gel electrophoresis as previously reported [11, 16]. Trypsin-digested phosphopeptides from whole lysates were enriched using Ga³⁺/TiO₂ immobilized metal ion chromatography. Eluted phosphopeptides were analyzed using MALDI-TOF-TOF and ESI MS/MS. Serine, threonine, and tyrosine phosphorylations were confirmed by phospho-Western blotting analysis.

2.2 ARPE-19 and HRP cells

For *in vitro* experiments, retinal pigment epithelial cells (ARPE-19) were purchased from ATCC (Manassas, VA) and retinal progenitor cells (HRP) were kindly donated by Dr. Harold J. Sheeldo at the University of North Texas Health Science Center. ARPE-19 and HRP cells were cultured in a 5% CO₂ incubator at 37°C in 100-mm dishes (Nalge Nunc International, Naperville, IL) using Dulbecco's modified Eagle's medium (DMEM) with fetal bovine serum (10%) and penicillin/streptomycin (1%). Confluent cells were trypsinized (5–7 min at 37°C) using a trypsin-EDTA buffer (0.1%, Sigma-Aldrich, St. Louis, MO), followed by centrifugation (300× g, 7 min). Cells (eight to nine passages) were grown to confluence for 2–4 days and then were treated with H₂O₂ (200 μM), intense light (7000–10,000 lux, 1–24 h) or constant light (700 lux, 48 h). Then, cells were rinsed (Modified Dulbecco's PBS) and lysed using IP lysis buffer containing Tris (25 mM), NaCl (150 mM), EDTA (1 mM), NP-40 (1%), glycerol (5%), and protease inhibitor cocktail at pH 7.4 by incubating on ice for 5 min with periodic sonication (3 × 5 min), followed by centrifugation (13,000× g, 10 min). Proteins (1 mg/ml, 200–400 μl) were loaded for immunoprecipitation and nonspecific bindings were avoided using control agarose resin cross-linked by 4% bead agarose. Amino-linked protein-A beads were used to immobilize antiprohibitin antibody with a coupling buffer (1 mM sodium phosphate, 150 mM NaCl, pH 7.2), followed by incubation (room temperature, 2 h) with sodium cyanoborohydride (3 μl, 5 M). Columns were washed using a washing buffer (1 M NaCl), and protein lysate was incubated in the protein A-antibody column with gentle rocking overnight at 4°C. The unbound proteins were spun down as flow-through, and the columns were washed three times using washing buffer to remove nonspecific binding proteins. The interacting proteins were eluted by incubating with elution buffer for 5 min at RT. The eluted proteins were equilibrated with Laemmli sample buffer (5X, 5% β-mercaptoethanol). Eluted proteins were separated using SDS-PAGE and stained using Coomassie blue (Pierce, IL) or silver staining kit (Bio-Rad, Hercules, CA). Immunoprecipitated proteins were reported previously [10] and were used to establish interactome in the current study.

2.3 *In vivo* oxidative stress

Constant light experiment was conducted as previously reported [21]. Female C₃HeB/FeJ mice (12 weeks of age) were purchased from the Jackson Laboratory (Bar Harbor, ME) and housed under a 12-h light/12-h dark cyclic lighting condition

(250–300 lux of full spectra fluorescent room light) for 2 weeks. The first group of mice (light/dark group) was housed in the 12-h light/12-h dark condition and the second group (constant light group) was housed in constant room light (250–300 lux) for 7 days. After euthanasia, eyes were rapidly removed from animals and retinas were isolated by microscopic dissection. Retinas were then washed with a solution of 250 mM sucrose, 10 mM Tris–HCl, at pH 7.0 to remove contaminants before lysis in 30 mM Tris–HCl, 2 M thiourea, 7 M urea, 4% CHAPS, and protease inhibitors. Samples were then sonicated intermittently until cells were lysed. The crude lysate was centrifuged at $20817\times g$ for 30 min at 4°C. Two-dimensional polyacrylamide gel electrophoresis (2D-PAGE) was performed using Ettan IPGphor system with 11 cm of immobilized pH gradient (IPG) strips (pH 5–8, ReadyStrip, Biorad) and 8–16% gradient Precast Gel (Criterion Precast Gel, Biorad). About 200 µg of retinal proteins were diluted to 200-µl solution with rehydration buffer (4% CHAPS, 8 M urea, 1% pharmalytes 3–10, 10 mM DTT). The mixture (200 µl) was incubated with IPG strip at room temperature for 30 min. IPG strips were rehydrated for 14 h at 30 V, followed by isoelectric focusing (IEF) performed at 500 V for 1 h, 500–8000 V for 6 h, and 8000 V for 1 h. After IEF, IPG strips were equilibrated for 15 min in 10-ml equilibration buffer containing 50 mM Tris–HCl (1.5 M, pH 8.8), 6 M urea, 30% glycerol (v/v), 2% SDS (w/v), trace amount of Bromophenol Blue, and 0.05 g DTT, and then re-equilibrated for another 15 min in the same buffer containing 0.45 g of iodoacetamide. Equilibrated strips were then placed on top of precast gradient gels and embedded in 0.5% agarose. Proteins were electrophoresed at 100 volts for about 2 h until the dye had reached the bottom of the gel. After electrophoresis, separated proteins were visualized using Coomassie blue staining. The Coomassie blue-stained gels were scanned with a transmission scanner and differential protein expression was analyzed. Differentially expressed protein spots were excised from gels and analyzed by MALDI-TOF and the selected proteins were further analyzed by MALDI-TOF-TOF mass spectrometry. All experiments were repeated in triplicate.

2.4 Protein identification by MALDI-TOF and TOF-TOF mass spectrometry

Protein spots, manually excised from the gel, were de-stained with 100 mM NH_4HCO_3 /50% acetonitrile (MeCN) at 37°C for 45 min twice. Gel slices were then incubated with 100% MeCN at room temperature for 5 min. After dehydration and drying, gel slices were incubated with 250 ng of trypsin (20 µg/20 µl, Promega) in 40 mM NH_4HCO_3 /10% MeCN at 37°C overnight. Trypsin/digestion buffer (50 µl) was added so that the gel slices were completely covered. After trypsin treatment, peptides were collected and gel slices were washed for 1 h with extraction buffer (50% MeCN, 0.1% Trifluoroacetic acid (TFA)) with gentle agitation. Peptides were combined and concentrated in a speed vacuum. Ziptip has been used to purify peptides. About 0.6 µl of purified peptides were mixed with 0.6 µl of alpha-Cyano-4-hydroxy-cinnamic acid matrix solution saturated in 50% MeCN/0.1% TFA solution (1:1 vol/vol) onto a MALDI 100-well target plate. It was analyzed through matrix-assisted laser/desorption ionization time of flight mass spectrometry (Bruker Ultraflex MALDI-TOF-TOF Mass spectrometer) in a reflector mode. Mass spectra and tandem mass spectra were acquired manually with laser intensity at 2400 and 200 shots per spectrum in MS mode and laser intensity at 3800 and 400 shots in MS/MS mode. The spectra were analyzed using Flex analysis 2.0 and Biotools 2.2 software. Peptide mass was calibrated internally using two trypsin auto digest ions (m/z 842.509, m/z 2211.104). Protein identification was performed using Mascot software (www.matrixscience.com) to search the National Center for Biotechnology Information (NCBI) database with mouse taxonomy. A missed trypsin cleavage was not allowed and 100 ppm of mass tolerance was applied for the search for the matching peptide.

For MALDI-TOF and peptide fingerprinting, the probability-based Mowse score is used $-10 \cdot \log(P)$, where P is the probability that the observed peptide match is a random event. Protein scores greater than 55 are considered significant ($p < 0.05$).

2.5 Immunocytochemical analysis

Cells were grown on sterile glass cover slips using DMEM/F12 medium with 10% FBS and 1% penicillin/streptomycin (Hyclone) in 5% CO₂ incubator at 37°C. Cells were treated under oxidative stress or intense light as previously reported [9–11, 18–20]. Cells were washed with PBS and incubated with MitoTracker Orange CMTMRos (100 nM, Molecular Probes, Carlsbad, CA) in serum-free culture medium (30 min, 37°C), followed by washing (PBS) and fixing (10% formaldehyde, 30 min, room temperature). Next, cells were treated using Triton X-100 (0.2%, Sigma-Aldrich, St. Louis, MO) in PBS (30 min) for permeabilization and blocked using complete medium (10% FBS, 0.05% Tween-20, 1 h). To stain cells, anti-actin, anti-tubulin, anti-vimentin antibody (1:100; Santa Cruz), and anti-prohibitin antibody (1:500, Genemed Synthesis Inc., San Antonio, TX, overnight, 4°C) were used; then, the cells were washed with PBS, followed by incubation with Alexa Fluor 488-conjugated anti-rabbit IgG secondary antibody (1:700; Molecular Probes, Carlsbad, CA, 1 h, room temperature). VECTASHIELD medium with DAPI (4,6-diamidino-2-phenylindole, the nucleus) was applied to mount the samples which were visualized using a Zeiss AxioVert fluorescent microscope (200 M Apo Tome, 63× magnification). Images were analyzed using ImageJ software (NIH).

2.6 AMD interactome map

Oxidative biomarker and AMD interactome were established using protein-protein interaction map software and databases, including STRING 10.0 (<http://string-db.org/>), MIPS (<http://mips.helmholtz-muenchen.de/proj/ppi/>), and iHOP (<http://www.ihop-net.org/UniPub/iHOP/>). Proteins found in AMD or oxidative stress conditions were added to establish the AMD interactome. Protein interactions were presented using eight categories, including neighborhood (green), gene fusion (red), co-occurrence (dark blue), co-expression (black), binding experiments (purple), databases (blue), text mining (lime), and homology (cyan). Protein interactions were determined and confirmed by genomic context, high-throughput experiments, co-expression, and previous publications in Pubmed. Protein database analysis showed the region-specific phosphorylation of specific proteins in AMD eyes. The AMD interactome was compared to the retina/RPE proteome under stress conditions.

3. Results

First, we determined the phosphorylation reactions in AMD samples to understand mitochondrial signaling, immune response, energy metabolism, and apoptosis under oxidative stress. The molecular network of altered phosphorylation is essential for determining molecular targets to treat AMD in the early stage. We built a comprehensive interaction map by combining several independent sets of *in vivo* and *in vitro* data including immunoprecipitation, co-expression, and protein domain information. The analysis of a large-scale phosphorylation reaction demonstrated that multiple phosphorylation motifs were implicated in the progression of AMD. A combination of phosphopeptide enrichment, high-performance liquid chromatography, and electrospray (ES)/time-of-flight (TOF) tandem mass spectrometry, followed by database search, provided an integrated

phosphoproteome showing that the apoptotic pathway, energy metabolism, inflammation, cytoskeletal rearrangement, and mitochondrial dysfunction were involved in AMD mechanism (**Figure 1**).

The AMD interactome was connected together using phosphoproteomics data from AMD tissues, *in vivo* murine model, and *in vitro* data from ARPE-19 cells. STRING 10.0 software was used to establish the protein interaction map to analyze the molecular mechanisms involved in AMD progression in terms of oxidative stress, inflammation switch, energy metabolism, and transcriptional regulation. The interactome map demonstrated that four distinguished subnetworks may exist in AMD: (A) complement activation by SERPING1, transferrin, albumin, and HFE, which are connected to vimentin/vitronectin/plasminogen/matrix metalloproteinase 2 (MMP2); (B) transcriptional regulation by hypoxia signaling, which is connected to angiogenesis, vascularization switch as well as apoptosis involving ubiquitin downstream; (C) mitochondrial signaling through ATP synthase, PPA1, VDAC2, PRDX2, mitofilin (IMMT), and prohibitin; and (D) apoptosis/mitotic spindle checkpoint/NOTCH signaling by caspase, MAD, BUB 1/3, NOTCH/ZWINT, and cyclin-dependent kinases (CDC).

The AMD interactome with oxidative biomarkers demonstrated that several proteins that were previously characterized as unrelated to AMD, including ubiquitin, peroxiredoxin, MAP kinase, BUB 1/3, vimentin, and crystalline, were involved

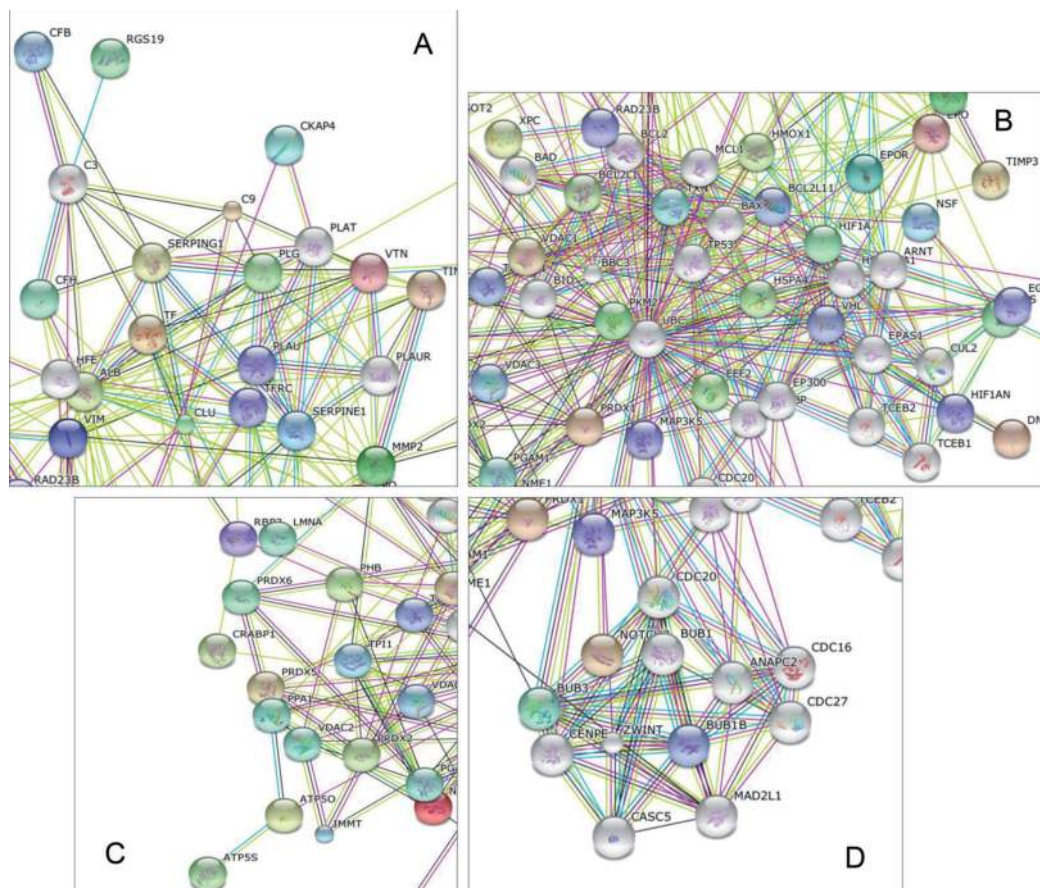


Figure 1. Mechanistic dissection of AMD using the AMD biomarker interactome from proteomics data. AMD biomarkers from *in vivo* experiments using postmortem AMD eyes are connected using STRING software, followed by adding proteomics data from murine model *in vivo* and ARPE19 cells *in vitro*. The whole map was divided into four subnetworks presenting complement activation (A); transcriptional regulation including angiogenesis, vascularization, apoptosis (B); mitochondrial network (C); and apoptosis/mitotic spindle checkpoint/NOTCH signaling (D).

in AMD progression. Our interactome map suggests that mitochondrial protein trafficking, crystalline aggregation, and protein degradation may contribute to AMD pathway. To confirm oxidative stress biomarkers, specific cytoskeletal protein changes were determined *in vivo* using an animal model under constant light (C₃H female mice, 7 weeks old, 7 days of light). Results from mass spectrometry analysis showed that neurofilament, vimentin, and β -tubulin were up-regulated under 24 h of constant light compared to 12-h dark/12-h light condition (**Figure 2**).

Based on our proteomics data showing altered signaling of apoptosis in the retina and RPE, new targets for anti-apoptotic and anti-angiogenic therapy can be determined. The current interactome suggests the new biomarkers and targets in AMD including: (1) mitochondrial dysfunction in the peripheral RPE (depleted prohibitin, increased ATP synthase); (2) oxidative stress including intense and constant light (peroxiredoxin, thioredoxin, glutathione S-transferase); (3) cytoskeletal/mitochondrial remodeling by microtubule, actin filament, and intermediate filament (tubulin, actin, vimentin); (4) high concentration of nitric oxide (nitric oxide synthase); (5) hypoxia responses (HIF1, erythropoietin, VEGF); (6) disrupted circadian clock (melatonin); (7) apoptotic downstream (pJAK2, pSTAT3, Bclxl, caspases); (8) altered lipid concentrations (cardiolipin, cholesterol); (9) altered visual cycle (CRABP, CRALBP, RPE65); (10) altered energy metabolism (S/T vs. Y kinases, carnitine, pyruvate, ATP synthase); (11) aggregation of heat shock proteins and crystallins; and (12) inflammation switch (CFH, C3, collagen, vitronectin).

Next, we examined light-induced protein regulation to determine oxidative stress biomarkers *in vivo*. Unbiased proteomic approaches, including 2D electrophoresis and mass spectrometry analysis were used. Upregulated tubulin beta4/5 and vimentin were found under constant light (24 light) compared to 12-h light/12-h dark *in vivo*. Their up-regulation in constant light-exposed retina is possibly due to hyperphosphorylation of tubulin/vimentin and increased apoptosis. Melatonin mediated downregulation of PP2A, which may stabilize vimentin and negatively regulated apoptosis to protect retina from light-induced damages (data not shown).

To determine the interdependence of mitochondrial trafficking versus oxidative stress, we examined β -tubulin and vimentin dynamics under stress conditions (**Figure 3A**). Constant or intense light accelerated β -tubulin aggregation as well as nuclear localization. Mitochondrial trafficking was colocalized with tubulin polymerization, whereas vimentin was more likely to determine mitochondrial morphology in the dark. Intense light also led to actin filament aggregation in cytosol in

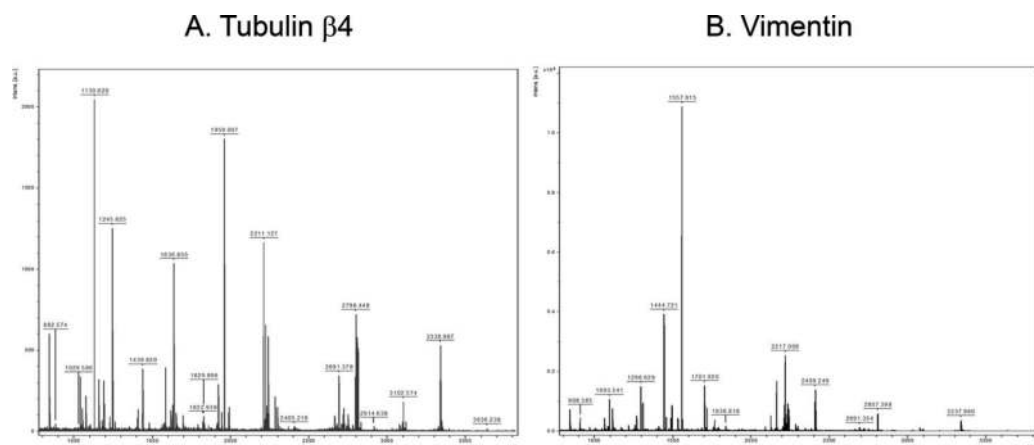


Figure 2. Identification of β -tubulin (A) and vimentin (B) by MALDI-TOF-TOF spectrometry analysis. Proteins were separated from mouse retina using 2D electrophoresis under constant light (24 light) group compared to control group (12 h light/12 h dark). β -tubulin and vimentin were up-regulated under constant light *in vivo*.

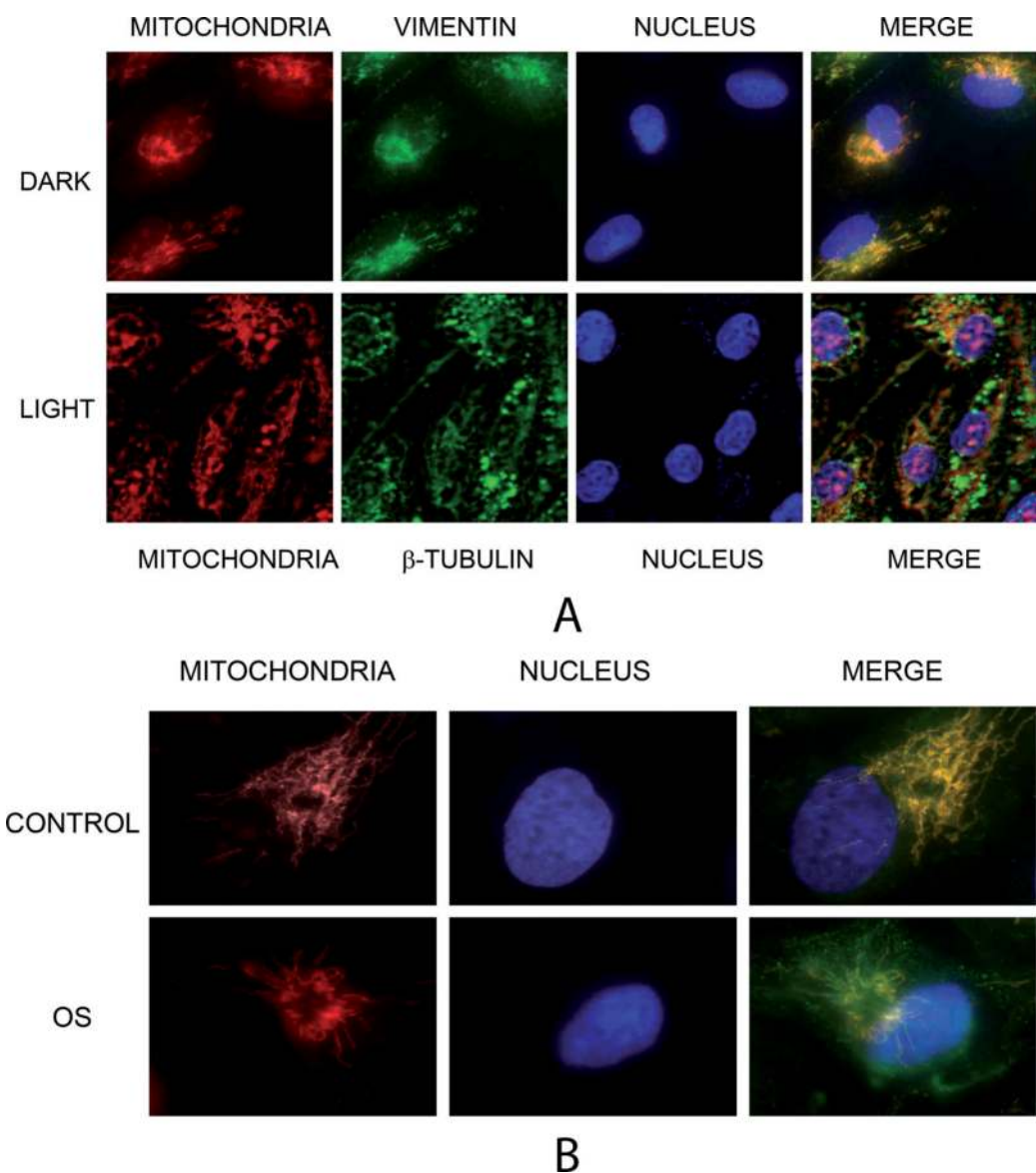


Figure 3. Immunocytochemistry of mitochondrial trafficking using tubulin, vimentin, and prohibitin. β -tubulin and vimentin dynamics under stress conditions were analyzed (panel A). Constant or intense light accelerated β -tubulin aggregation as well as nuclear localization. Mitochondrial trafficking was colocalized with tubulin polymerization, whereas vimentin determines mitochondrial morphology in the dark. Vimentin was shown as an extended filamentous structure in control; however, it was aggregated around the nucleus under intense light (7000 lux). Mitochondrial prohibitin moved into the nucleus under intense light or oxidative stress (panel B).

the RPE. Cytosolic β -actin in the dark entered the nucleus under stress conditions. Immunocytochemistry of tubulin and actin demonstrated oxidative stress-mediated mitochondrial aggregation and size changes along with mitochondrial decay. Vimentin was shown as an extended filamentous structure in control; however, it was aggregated around the nucleus under stress conditions, that is oxidative stress and intense light (7000 lux). Mitochondrial proteins and cytoskeletal proteins, including prohibitin, actin, tubulin, and vimentin moved toward the nucleus under oxidative stresses (**Figure 3B**).

Translocation of prohibitin might be related to post-transcriptional regulation and mitochondrial membrane depolarization. Down- or up-regulation of prohibitin in specific concentrations of H_2O_2 may imply one of several anti-apoptotic or pro-apoptotic responses depending on the intensity and temporal pattern of

the stress. In our previous experiment, NF- κ B was translocated into the nucleus in oxidative stress as a survival factor. It is important to note that prohibitin and NF- κ B moved in parallel or opposite directions between the nucleus and mitochondria under various conditions. This coordinated translocalization may determine cell viability and apoptotic population in the retina and RPE.

We also examined the nuclear function of prohibitin by immunoprecipitation. Prohibitin binds with many transcription factors and nucleotide-binding proteins, including TFIIB, DNA mismatch repair protein, ski2-type helicase, Cyclin-D-binding Myb-like transcription factor 1, DNA ligase, elongation factor, and BRCA1-A complex subunit RAP80. Additional interacting proteins have been reported such as E2F, retinoblastoma-associated protein, cellular tumor antigen p53, Heatshock 70: Stress-70 protein, and histone deacetylase (HDAC1). We confirmed transcriptional regulation of prohibitin by immunoprecipitation and protein-nucleotide binding assay.

Next, we established the signaling network of AMD using the interactome results. Based on our proteomics and interactome data, the potential AMD mechanisms were integrated as shown in **Figure 4**, suggesting altered energy metabolism, mitochondrial dysfunction, retinoid metabolism, circadian clock, inflammation, angiogenesis, lipid metabolism, and apoptosis.

Previous data demonstrated that Hsp70 (c-Jun N-terminal kinase), crystallins (Akt), and the increased expression of VDAC might be involved in AMD progression [22–26]. Altered phosphorylations of mitochondrial heat shock protein mtHsp70, α A/ α B crystalline, vimentin, and ATP synthase were observed in RPE cell death under oxidative stress [9, 22, 27–29]. Retinoid-binding proteins, including CRABP, RPE65, and RLBP1, could be involved in the advanced stages of AMD [30–32]. It was reported that accumulation of all-*trans*-retinal (atRAL), an important intermediate of the visual cycle, led to NADPH (reduced nicotinamide adenine dinucleotide phosphate) activation, resulting in ROS production and apoptosis of RPE cells [33–37]. Therefore, atRAL can play an important role in AMD pathogenesis, and its action can be underlined by oxidative stress, which can be potentiated by mitochondrial impairment; however, it is elusive whether dysfunctions in atRAL clearance belong to the initiation or consequence of AMD [35–37].

We observed altered lipid compositions that include increased carbon number of fatty acids, double bond saturation, higher cholesterol, and phosphatidylcholine, whereas cardiolipin levels decreased in RPE apoptosis [9, 10, 18]. Changes in lipid concentrations seem to diminish the membrane fluidity and accelerate protein aggregation in the RPE [38–44].

In vivo data demonstrated that PP2A and vimentin are modulated by constant light and are key elements involved in cytoskeletal signaling in rd1 mutation model [19, 45, 46]. The expression levels of vimentin and PP2A are significantly increased when C₃HeB/FeJ mice (rd1 allele; 12 weeks; photoreceptors degenerated) are exposed under continuous light for 7 days compared to a condition of 12-h light/dark cycling exposure. When melatonin is administered to animals while they are exposed to continuous light, the increased levels of vimentin and PP2A return to a normal level. Further, vimentin has been shown to be a target of PP2A that directly binds vimentin and dephosphorylates it. Vimentin is present in all mesenchymal cells, and often used as a differentiation marker. Like other intermediate filaments, vimentin acts to maintain cellular integrity; however, vimentin phosphorylation level determines RPE survival by the polymerization/depolymerization mechanism.

A positive correlation between the levels of PP2A and vimentin under light-induced stress suggests that cytoskeletal dynamics are regulated by vimentin phosphorylation. We postulate that light may induce post-translational modifications of vimentin. Stabilized vimentin may act as an anti-apoptotic agent when cells are under stress.

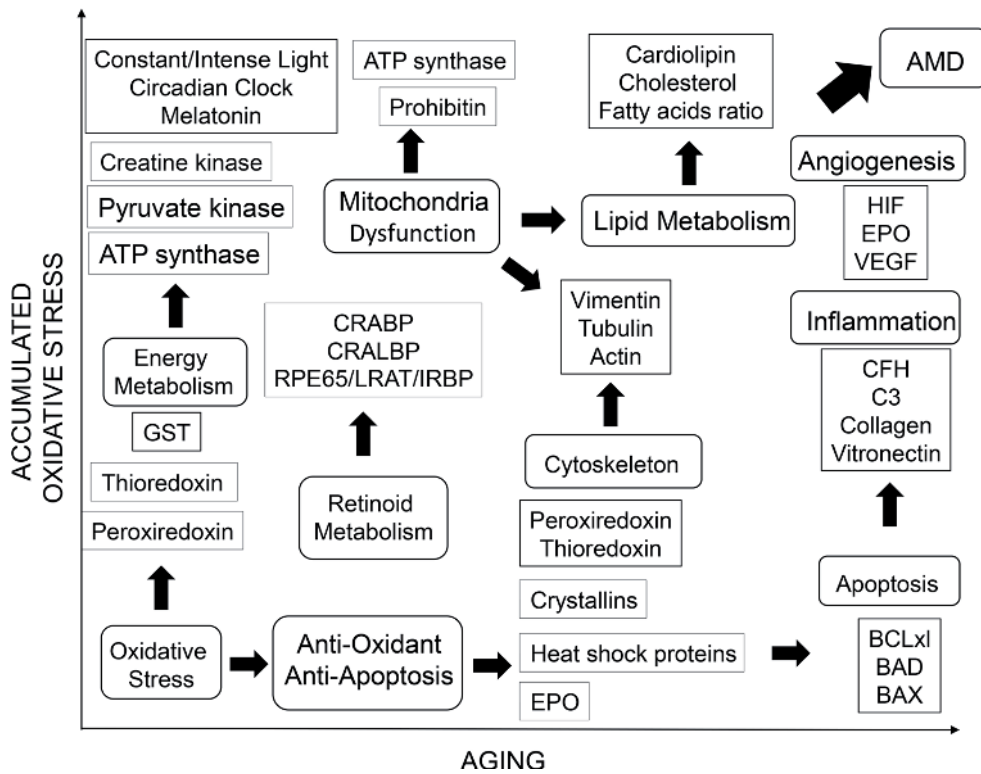


Figure 4. AMD interactome and mechanistic dissection of AMD interpreted by phosphorylation reactions. Phosphoproteome alterations in the retina and RPE may lead to the pathological pathway which would be suited as targets for anti-apoptotic and anti-angiogenic therapy in AMD: (1) mitochondrial dysfunction in the peripheral RPE; (2) oxidative stress including intense and constant light; (3) cytoskeletal remodeling by actin, tubulin, and vimentin; (4) high concentration of nitric oxide; (5) hypoxia; (6) disrupted circadian clock; (7) apoptotic pathway through pJAK2, pSTAT3, Bclxl; (8) altered lipid concentrations; (9) altered visual cycle; (10) altered energy metabolism (ATP synthase, carnitine kinase, pyruvate kinases); (11) aggregation of heat shock proteins and crystallins, and inflammation (CFH, C3, collagen, vitronectin). Based on our proteomics data, we tested the following anti-apoptotic or anti-angiogenic molecules: (1) prohibitin (anti-apoptotic mitochondrial-nuclear shuttle); (2) erythropoietin as an anti-apoptotic protein via JAK2/STAT3 pathway; (3) melatonin as an anti-apoptotic and anti-angiogenic molecule protecting cytoskeletal reorganization through PP2A/vimentin pathway; (4) okadaic acid, arginine, and SNAP to control nitric oxide concentration; (5) cardiolipin and cholesterol; (6) anthocyanin (anti-angiogenic via VEGFR2 pathway); (7) phospholipids, fatty acids, cyclodextrin to control lipids and cholesterol concentration.

The current interactome suggests that altered phosphoproteome interactions, including pyruvate kinase, tyrosine kinase, and vimentin, exist in the retina and RPE in AMD. Phospho-Western blotting analysis revealed that phosphorylations of intermediate filament vimentin (Ser38, Ser55) and mitochondrial heat shock protein mtHsp70 were modulated in the RPE *in vitro* [9, 19, 22, 28, 47]. Changes of vimentin phosphorylation are directed to reorganization of the intermediate filament network and altered function of RPE cells.

4. Discussion

We used bioinformatics approaches to integrate molecular events associated with the progression of AMD. Proteomics data obtained using the oxidative stress animal model as well as the *in vitro* model were combined with previous AMD interactome results. We highlighted the importance of mitochondrial and cytoskeletal proteins in the oxidative stress responses in AMD models, including prohibitin, tubulin, and vimentin. In addition, we used immunocytochemistry

analysis to validate the AMD interactome data, showing that mitochondria moved to the nucleus under intense light or oxidative stress conditions possibly through the tubulin/vimentin filament reorganization mechanism.

The current interactome mapping also suggests that changes in phosphoprotein levels in response to oxidative stress may induce complement activation, transcriptional regulation, mitochondrial dysfunction, and apoptosis. The phosphorylation signaling may explain why AMD is induced by oxidative stress and how the downstream of phosphorylations are associated with the changes of mitochondrial protein expressions, cytoskeleton reorganization, membrane remodeling, and lipid oxidation. For example, previous observations of vimentin derived from human choroidal neovascular membranes in AMD, as well as in drusen and melanolipofuscin, support the positive correlation between the biomarkers we characterized in RPE cells under stress and the AMD proteomics.

The AMD interactome map also elucidates the regulatory mechanism of apoptotic cell death governed by phosphorylation. Changes in the global phosphoproteome could be one of indications of early signaling events, including an increase of longer chain fatty acids, especially phosphatidylcholine and cholesteryl esters. The phosphoprotein interactome also provides a connection between oxidative stress-induced mitochondrial trafficking changes and AMD.

We also emphasize that mitochondria play a significant role in stress response in RPE cells, and this in turn influences the progression of AMD. The number of RPE mitochondria decreases with aging [48]. Through the observation by scanning electron microscope, mitochondrial shape becomes more oval in normal aged samples, while it is more bacillus-like in young eyes. The number of cristae decreases and cristae structure is less organized in aged tissue. In addition, mitochondrial matrix shows less electron density along with aging. In AMD samples, loss of cristae structure and matrix density is more obvious. Bleb formation on mitochondrial membrane and loss of mitochondrial membrane integrity were also observed in AMD [32, 49, 50].

Previously, quantitative analysis of mitochondrial morphology reveals that mitochondrial structure and functionality are closely associated with aging and AMD [9, 22, 32, 51–57]. In both aging and AMD samples, mitochondrion number per cell, cristae per mitochondrion, and mean area of mitochondrion per cell are declined. A similar trend was also observed in oxidative stressed ARPE-19, where mitochondrial distribution also changed. It is important to note that a mitochondrion is a highly dynamic organelle in response to different environmental factors, and those responses may determine the cell fate. RPE mitochondria undergo loss of structural integrity under oxidative stress and aging, indicating that mitochondrial signaling could be interrupted in AMD.

The retrograde communication from mitochondria to the nucleus has been demonstrated by our previous data by tracking the chaperon protein prohibitin using fluorescent microscopy techniques [10, 18, 58]. Mitochondrial components may also determine cell signaling in the nucleus, including change of mitochondrial membrane potential, mitochondrial DNA (mtDNA), and mitochondrial protein expressions. When cumulative damages hit the threshold where mitochondria cannot maintain their structural integrity, there is a decrease of mitochondrial membrane potential, along with a number of mitochondrial components released into the cytosol, including cardiolipin, cytochrome c, and Ca^{2+} . Release of cytochrome c initiates the caspase-dependent apoptosis and triggers more Ca^{2+} release from endoplasmic reticulum, whereas elevation of cytosolic Ca^{2+} level can cause more cytochrome c release and activation of caspase-9.

Mitochondrial DNA (mtDNA) is susceptible to oxidative stress damage. Compared to nuclear DNA (nDNA), mtDNA is located in mitochondrial matrix in close proximity to the ROS source in the cell. MtDNA is lack of histones and

contains no introns that also increases its susceptibility to oxidative damage. Meanwhile, mtDNA mainly encodes electron transport chain proteins, including ATP synthase, cytochrome b, cytochrome c oxidase, and NADH dehydrogenase. Damaged mtDNA will lead to impaired electron transport chain proteins, further deteriorating cell energy production, generating more ROS, and inducing extra damages to mtDNA. Previous studies have revealed that abnormal mtDNA leads to reduced energy production and initiation of apoptosis [59–62]. Loss of mtDNA in ARPE-19 cells led to the change of nuclear gene expression, especially the up-regulation of genes related to glycolysis [63–65].

The mitochondrial-nuclear crosstalk could be a mechanism that the RPE cell uses to compensate the insufficient energy productions due to the mitochondrial dysfunction. Other changes in nuclear gene expressions caused by loss of mtDNA include up-regulation of proteins related to uptake of ROS and drusen, extracellular matrix and matrix enzymes, lipid transport-related proteins, and inflammation-related regulators. Therefore, damaged mtDNA has been considered as an important biomarker of oxidative stressed RPE and progression of AMD [50, 66, 67]. Fragments of mtDNA have been found to migrate to the nucleus and be inserted into the nuclear genome [68–71]. The entrance of mitochondria into the nucleus has been reported to promote both the attack of mitochondria by nuclear protein and the attack of nuclear DNA and protein by protein of the mitochondrial intermembrane space [65, 68–74]. Mitochondria move to the nucleus under stress to fulfill energy demand of the nucleus. Therefore, our observation that mitochondria entering the nucleus could be one of the mechanisms to explain mitochondrial diseases and the aging process.

Our AMD interactome map implies that a positive correlation exists between AMD mechanism and early oxidative stress biomarkers, as well as inflammation switch, apoptosis, transcriptional regulation, and mitochondrial dysfunction [26, 32, 52, 75–77]. The mechanistic dissection of our AMD interactome map is the initial delineation of the underlying physiology of oxidative stress-mediated phosphorylation signaling in RPE apoptosis which can lead to AMD progression. In addition, the phosphoprotein interactome provides a stimulus for understanding oxidative stress-induced mitochondrial changes and the mechanism of aggregate formation induced by protein phosphorylations. As a consequence, an effective therapeutic approach to treat AMD based on the modulation of phosphorylation reactions is expected to result.

Author details

Weilue He¹, Srinivas R. Sripathi², Madu Joshua³, Ruonan Zhang⁴, Fabunmi Tosin³, Patrick Ambrose³, Diana R. Gutsaeva⁵ and Wan Jin Jahng^{3*}

1 Department of Biomedical Engineering, Michigan Technological University, Houghton, MI, USA

2 Department of Ophthalmology, Wilmer Eye Institute, The Johns Hopkins University School of Medicine, Baltimore, MD, USA


3 Retina Proteomics Laboratory, Department of Petroleum Chemistry, American University of Nigeria, Yola, Adamawa, Nigeria

4 Department of Ophthalmology, University of South Carolina, Columbia, SC, USA

5 Department of Ophthalmology, Augusta University, Augusta, GA, USA

*Address all correspondence to: wan.jahng@aun.edu.ng

IntechOpen

© 2019 The Author(s). Licensee IntechOpen. This chapter is distributed under the terms of the Creative Commons Attribution License (<http://creativecommons.org/licenses/by/3.0>), which permits unrestricted use, distribution, and reproduction in any medium, provided the original work is properly cited. 

References

- [1] Zarbin MA. Current concepts in the pathogenesis of age-related macular degeneration. *Archives of Ophthalmology* (Chicago, IL, 1960). 2004;**122**:598-614. DOI: 10.1001/archophth.122.4.598
- [2] Kanagasingam Y, Bhuiyan A, Abramoff MD, Smith RT, Goldschmidt L, Wong TY. Progress on retinal image analysis for age related macular degeneration. *Progress in Retinal and Eye Research*. 2014;**38**:20-42. DOI: 10.1016/j.preteyeres.2013.10.002
- [3] Edwards AO, Ritter R, Abel KJ, Manning A, Panhuysen C, Farrer LA. Complement factor H polymorphism and age-related macular degeneration. *Science*. 2005;**308**:421-424. DOI: 10.1126/science.1110189
- [4] Wu Z, Lauer TW, Sick A, Hackett SF, Campochiaro PA. Oxidative stress modulates complement factor H expression in retinal pigmented epithelial cells by acetylation of FOXO3. *The Journal of Biological Chemistry*. 2007;**282**:22414-22425. DOI: 10.1074/jbc.M702321200
- [5] Jiang M, Esteve-Rudd J, Lopes VS, Diemer T, Lillo C, Rump A, et al. Microtubule motors transport phagosomes in the RPE, and lack of KLC1 leads to AMD-like pathogenesis. *The Journal of Cell Biology*. 2015;**210**:jcb.201410112. DOI: 10.1083/jcb.201410112
- [6] Alcazar O, Hawkridge AM, Collier TS, Cousins SW, Bhattacharya SK, Muddiman DC, et al. Proteomics characterization of cell membrane blebs in human retinal pigment epithelium cells. *Molecular & Cellular Proteomics*. 2009;**8**:2201-2211. DOI: 10.1074/mcp.M900203-MCP200
- [7] Spencer KL, Olson LM, Anderson BM, Schnetz-Boutaud N, Scott WK, Gallins P, et al. C3 R102G polymorphism increases risk of age-related macular degeneration. *Human Molecular Genetics*. 2008;**17**:1821-1824. DOI: 10.1093/hmg/ddn075
- [8] Grimm C, Wenzel A, Hafezi F, Yu S, Redmond TM, Remé CE. Protection of Rpe65-deficient mice identifies rhodopsin as a mediator of light-induced retinal degeneration. *Nature Genetics*. 2000;**25**:63-66. DOI: 10.1038/75614
- [9] Sripathi SR, He W, Sylvester OD, Neksumi M, Um JY, Dluya T, et al. Altered cytoskeleton as a mitochondrial decay signature in the retinal pigment epithelium. *The Protein Journal*. 2016;**35**:179-192. DOI: 10.1007/s10930-016-9659-9
- [10] Sripathi SR, Sylvester O, He W, Moser T, Um J-Y, Lamoke F, et al. Prohibitin as the molecular binding switch in the retinal pigment epithelium. *The Protein Journal*. 2016;**35**:1-16. DOI: 10.1007/s10930-015-9641-y
- [11] Sripathi S, He W, Prigge CL, Sylvester O, Um J-Y, Powell FL, et al. Interactome mapping guided by tissue-specific phosphorylation in age-related macular degeneration. *International Journal of Scientific and Engineering Research*. 2017;**8**:680-698. DOI: 10.14299/ijser.2017.02.010
- [12] Xue L, Gollapalli DR, Maiti P, Jahng WJ, Rando RR. A palmitoylation switch mechanism in the regulation of the visual cycle. *Cell*. 2004;**117**:761-771. DOI: 10.1016/j.cell.2004.05.016
- [13] Jahng WJ. New Biomarkers in the Retina and RPE Under Oxidative Stress. *Ocular Diseases*, Adedayo Adio. Rijeka, Croatia: InTechOpen; 2012. DOI: 10.5772/1678
- [14] Chung H, Lee H, Lamoke F, Hrushesky WJM, Wood PA,

- Jahng WJ. Neuroprotective role of erythropoietin by antiapoptosis in the retina. *Journal of Neuroscience Research*. 2009;**87**:2365-2374. DOI: 10.1002/jnr.22046
- [15] Lee H, Chung H, Arnouk H, Lamoke F, Hunt RC, Hrushesky WJM, et al. Cleavage of the retinal pigment epithelium-specific protein RPE65 under oxidative stress. *International Journal of Biological Macromolecules*. 2010;**47**:104-108. DOI: 10.1016/j.ijbiomac.2010.05.014
- [16] Lee H, Chung H, Lee SH, Jahng WJ. Light-induced phosphorylation of crystallins in the retinal pigment epithelium. *International Journal of Biological Macromolecules*. 2011;**48**:194-201. DOI: 10.1016/j.ijbiomac.2010.11.006
- [17] Arnouk H, Lee H, Zhang R, Chung H, Hunt RC, Jahng WJ. Early biosignature of oxidative stress in the retinal pigment epithelium. *Journal of Proteomics*. 2011;**74**:254-261. DOI: 10.1016/j.jprot.2010.11.004
- [18] Sripathi SR, He W, Atkinson CL, Smith JJ, Liu Z, Elledge BM, et al. Mitochondrial-nuclear communication by prohibitin shuttling under oxidative stress. *Biochemistry*. 2011;**50**:8342-8351. DOI: 10.1021/bi2008933
- [19] Sripathi SR, He W, Um JY, Moser T. Nitric oxide leads to cytoskeletal reorganization in the retinal pigment epithelium under oxidative stress. *Advances in Bioscience and Biotechnology*. 2012;**03**:1167-1178. DOI: 10.4236/abb.2012.38143
- [20] Sripathi SR, Prigge CL, Elledge B, He W, Offor J, Gutsaeva DR, et al. Melatonin modulates prohibitin and cytoskeleton in the retinal pigment epithelium. *International Journal of Scientific and Engineering Research*. 2017;**8**:502-506. DOI: 10.14299/ijser.2017.07.001
- [21] Zhang R, Hrushesky WJM, Wood PA, Lee SH, Hunt RC, Jahng WJ. Melatonin reprogrammes proteomic profile in light-exposed retina in vivo. *International Journal of Biological Macromolecules*. 2010;**47**:255-260. DOI: 10.1016/j.ijbiomac.2010.04.013
- [22] Nordgaard CL, Karunadharma PP, Feng X, Olsen TW, Ferrington DA. Mitochondrial proteomics of the retinal pigment epithelium at progressive stages of age-related macular degeneration. *Investigative Ophthalmology & Visual Science*. 2008;**49**:2848-2855. DOI: 10.1167/iovs.07-1352
- [23] Nakata K, Crabb JW, Hollyfield JG. Crystallin distribution in Bruch's membrane-choroid complex from AMD and age-matched donor eyes. *Experimental Eye Research*. 2005;**80**:821-826. DOI: 10.1016/j.exer.2004.12.011
- [24] Crabb JW, Miyagi M, Gu X, Shadrach K, West KA, Sakaguchi H, et al. Drusen proteome analysis: An approach to the etiology of age-related macular degeneration. *Proceedings of the National Academy of Sciences of the United States of America*. 2002;**99**:14682-14687. DOI: 10.1073/pnas.222551899
- [25] Umeda S, Suzuki MT, Okamoto H, Ono F, Mizota A, Terao K, et al. Molecular composition of drusen and possible involvement of anti-retinal autoimmunity in two different forms of macular degeneration in cynomolgus monkey (*Macaca fascicularis*). *The FASEB Journal*. 2005;**19**:1683-1685. DOI: 10.1096/fj.04-3525fje
- [26] Nita M, Grzybowski A, Ascaso FJ, Huerva V. Age-related macular degeneration in the aspect of chronic low-grade inflammation (pathophysiological parainflammation). *Mediators of Inflammation*. 2014;**2014**:930671. DOI: 10.1155/2014/930671

- [27] Aoki H, Hara A, Nakagawa S, Motohashi T, Hirano M, Takahashi Y, et al. Embryonic stem cells that differentiate into RPE cell precursors in vitro develop into RPE cell monolayers in vivo. *Experimental Eye Research*. 2006;**82**:265-274. DOI: 10.1016/j.exer.2005.06.021
- [28] Kaempfer S, Walter P, Salz AK, Thumann G. Novel organotypic culture model of adult mammalian neurosensory retina in co-culture with retinal pigment epithelium. *Journal of Neuroscience Methods*. 2008;**173**:47-58. DOI: 10.1016/j.jneumeth.2008.05.018
- [29] Huang H, Li F, Alvarez RA, Ash JD, Anderson RE. Downregulation of ATP synthase subunit-6, cytochrome c oxidase-III, and NADH dehydrogenase-3 by bright cyclic light in the rat retina. *Investigative Ophthalmology & Visual Science*. 2004;**45**:2489-2496. DOI: 10.1167/iovs.03-1081
- [30] Lakkaraju A, Finnemann SC, Rodriguez-Boulan E. The lipofuscin fluorophore A2E perturbs cholesterol metabolism in retinal pigment epithelial cells. *Proceedings of the National Academy of Sciences of the United States of America*. 2007;**104**:11026-11031. DOI: 10.1073/pnas.0702504104
- [31] Yuan X, Gu X, Crabb JSW, Yue X, Shadrach K, Hollyfield JG, et al. Quantitative proteomics: Comparison of the macular Bruch membrane/choroid complex from age-related macular degeneration and normal eyes. *Molecular & Cellular Proteomics*. 2010;**9**:1031-1046. DOI: 10.1074/mcp.M900523-MCP200
- [32] Suter M, Remé C, Grimm C, Wenzel A, Jäätela M, Esser P, et al. Age-related macular degeneration: The lipofuscin component N-retinyl-N-retinylidene ethanolamine detaches proapoptotic proteins from mitochondria and induces apoptosis in mammalian retinal pigment epithelial cells. *The Journal of Biological Chemistry*. 2000;**275**:39625-39630. DOI: 10.1074/jbc.M007049200
- [33] Zhu X, Wang K, Zhang K, Zhou F, Zhu L. Induction of oxidative and nitrosative stresses in human retinal pigment epithelial cells by all-trans-retinal. *Experimental Cell Research*. 2016;**348**:87-94. DOI: 10.1016/j.yexcr.2016.09.002
- [34] Wang H, Wittchen ES, Hartnett ME. Breaking barriers: Insight into the pathogenesis of neovascular age-related macular degeneration. *Eye Brain*. 2011;**3**:19-28. DOI: 10.2147/EB.S24951
- [35] Mata NL, Tzekov RT, Liu X, Weng J, Birch DG, Travis GH. Delayed dark-adaptation and lipofuscin accumulation in *abcr*^{+/-} mice: Implications for involvement of ABCR in age-related macular degeneration. *Investigative Ophthalmology and Visual Science*. 2001;**42**:1685-1690
- [36] Ueda K, Zhao J, Kim HJ, Sparrow JR. Photodegradation of retinal bisretinoids in mouse models and implications for macular degeneration. *Proceedings of the National Academy of Sciences, United States of America*. 2016;**113**:6904-6909. DOI: 10.1073/pnas.1524774113
- [37] Zhang J, Kiser PD, Badiie M, Palczewska G, Dong Z, Golczak M, et al. Molecular pharmacodynamics of emixustat in protection against retinal degeneration. *The Journal of Clinical Investigation*. 2015;**125**:2781-2794. DOI: 10.1172/JCI80950
- [38] Wang L, Clark ME, Crossman DK, Kojima K, Messinger JD, Mobley J, et al. Abundant lipid and protein components of drusen. *PLoS One*. 2010;**5**:e10329. DOI: 10.1371/journal.pone.0010329
- [39] Nikolaeva O, Moiseyev G, Rodgers KK, Ma J-X. Binding to lipid membrane induces conformational changes in RPE65: Implications for

its isomerohydrolase activity. *The Biochemical Journal*. 2011;**436**:591-597. DOI: 10.1042/BJ20110091

[40] Bretillon L, Thuret G, Grégoire S, Acar N, Joffre C, Bron AM, et al. Lipid and fatty acid profile of the retina, retinal pigment epithelium/choroid, and the lacrimal gland, and associations with adipose tissue fatty acids in human subjects. *Experimental Eye Research*. 2008;**87**:521-528. DOI: 10.1016/j.exer.2008.08.010

[41] Yuan Q, Kaylor JJ, Miu A, Bassilian S, Whitelegge JP, Travis GH. Rpe65 isomerase associates with membranes through an electrostatic interaction with acidic phospholipid headgroups. *The Journal of Biological Chemistry*. 2010;**285**:988-999. DOI: 10.1074/jbc.M109.025643

[42] Trudel E, Beaufils S, Renault A, Breton R, Salesse C. Binding of RPE65 fragments to lipid monolayers and identification of its partners by glutathione S-transferase pull-down assays. *Biochemistry*. 2006;**45**:3337-3347. DOI: 10.1021/bi0519405

[43] Golczak M, Kiser PD, Lodowski DT, Maeda A, Palczewski K. Importance of membrane structural integrity for RPE65 retinoid isomerization activity. *The Journal of Biological Chemistry*. 2010;**285**:9667-9682. DOI: 10.1074/jbc.M109.063941

[44] Kopitz J, Holz FG, Kaemmerer E, Schutt F. Lipids and lipid peroxidation products in the pathogenesis of age-related macular degeneration. *Biochimie*. 2004;**86**:825-831. DOI: 10.1016/j.biochi.2004.09.029

[45] Turowski P, Myles T, Hemmings B, Fernandez NJ, Lamb, Vimentin dephosphorylation by protein phosphatase 2A is modulated by the targeting subunit B55. *Molecular Biology of the Cell*. 1999;**10**:1997-2015. Available from: <http://www>

pubmedcentral.nih.gov/articlerender.fcgi?artid=25403&tool=pmcentrez&rendertype=abstract

[46] Eriksson JE, He T, Trejo-Skalli AV, Härmälä-Braskén A-S, Hellman J, Chou Y-H, et al. Specific in vivo phosphorylation sites determine the assembly dynamics of vimentin intermediate filaments. *Journal of Cell Science*. 2004;**117**:919-932. DOI: 10.1242/jcs.00906

[47] Guidry C, Medeiros NE, Curcio CA. Phenotypic variation of retinal pigment epithelium in age-related macular degeneration. *Investigative Ophthalmology & Visual Science*. 2002;**43**:267-273. Available from: <http://www.ncbi.nlm.nih.gov/pubmed/11773041>

[48] He Y, Ge J, Burke JM, Myers RL, Dong ZZ, Tombran-Tink J. Mitochondria impairment correlates with increased sensitivity of aging RPE cells to oxidative stress. *Journal of Ocular Biology, Diseases, and Informatics*. 2010;**3**:92-108. DOI: 10.1007/s12177-011-9061-y

[49] Feher J, Kovacs I, Artico M, Cavallotti C, Papale A, Balacco Gabrieli C. Mitochondrial alterations of retinal pigment epithelium in age-related macular degeneration. *Neurobiology of Aging*. 2006;**27**:983-993. DOI: 10.1016/j.neurobiolaging.2005.05.012

[50] Liang F-QQ, Godley BF. Oxidative stress-induced mitochondrial DNA damage in human retinal pigment epithelial cells: A possible mechanism for RPE aging and age-related macular degeneration. *Experimental Eye Research*. 2003;**76**:397-403. DOI: 10.1016/S0014-4835(03)00023-X

[51] Markovets AM, Fursova AZ, Kolosova NG. Therapeutic action of the mitochondria-targeted antioxidant SkQ1 on retinopathy in OXYS rats linked

- with improvement of VEGF and PEDF gene expression. *PLoS One*. 2011;**6**:1-8. DOI: 10.1371/journal.pone.0021682
- [52] Terluk MR, Kapphahn RJ, Soukup LM, Gong H, Gallardo C, Montezuma SR, et al. Investigating mitochondria as a target for treating age-related macular degeneration. *The Journal of Neuroscience*. 2015;**35**:7304-7311. DOI: 10.1523/JNEUROSCI.0190-15.2015
- [53] Karunadharma PP, Nordgaard CL, Olsen TW, a Ferrington D. Mitochondrial DNA damage as a potential mechanism for age-related macular degeneration. *Investigative Ophthalmology & Visual Science*. 2010;**51**:5470-5479. DOI: 10.1167/iovs.10-5429
- [54] a Voloboueva L, Killilea DW, Atamna H, Ames BN. N-tert-butyl hydroxylamine, a mitochondrial antioxidant, protects human retinal pigment epithelial cells from iron overload: Relevance to macular degeneration. *The FASEB Journal*. 2007;**21**:4077-4086. DOI: 10.1096/fj.07-8396com
- [55] Paraoan L, Ratnayaka A, Spiller DG, Hiscott P, White MRH, Grierson I. Unexpected intracellular localization of the AMD-associated cystatin C variant. *Traffic*. 2004;**5**:884-895. DOI: 10.1111/j.1600-0854.2004.00230.x
- [56] Finley LWS, Haigis MC. The coordination of nuclear and mitochondrial communication during aging and calorie restriction. *Ageing Research Reviews*. 2009;**8**:173-188. DOI: 10.1016/j.arr.2009.03.003
- [57] Hoye AT, Davoren JE, Wipf P, Fink MP, Kagan VE. Targeting mitochondria. *Accounts of Chemical Research*. 2008;**41**:87-97. DOI: 10.1021/ar700135m
- [58] Lee H, Arnouk H, Sripathi S, Chen P, Zhang R, Bartoli M, et al. Prohibitin as an oxidative stress biomarker in the eye. *International Journal of Biological Macromolecules*. 2010;**47**:685-690. DOI: 10.1016/j.ijbiomac.2010.08.018
- [59] Tuppen HAL, Blakely EL, Turnbull DM, Taylor RW. Mitochondrial DNA mutations and human disease. *Biochimica et Biophysica Acta*. 2010;**1797**:113-128. DOI: 10.1016/j.bbabi.2009.09.005
- [60] Rudel T, Kepp O, Kozjak-Pavlovic V, Santhanam S, Venkatraman A, Ramakrishna BS, et al. Mitochondrial dysfunction and insulin resistance: An update. *Journal of Pediatric Gastroenterology and Nutrition*. 2014;**4**:1172-1184. DOI: 10.1007/s00535-009-0119-6
- [61] Kenney MC, Atilano SR, Boyer D, Chwa M, Chak G, Chinichian S, et al. Characterization of retinal and blood mitochondrial DNA from age-related macular degeneration patients. *Investigative Ophthalmology and Visual Science*. 2010;**51**:4289-4297. DOI: 10.1167/iovs.09-4778
- [62] Hill BG, Benavides GA, Lancaster JJR, Ballinger S, Dell'Italia L, Zhang J, et al. Integration of cellular bioenergetics with mitochondrial quality control and autophagy. *Biological Chemistry*. 2012;**393**:1485-1512. DOI: 10.1515/hsz-2012-0198
- [63] Gramajo AL, Zacharias LC, Neekhra A, Luthra S, Atilano SR, Chwa M, et al. Mitochondrial DNA damage induced by 7-ketocholesterol in human retinal pigment epithelial cells in vitro. *Investigative Ophthalmology & Visual Science*. 2010;**51**:1164-1170. DOI: 10.1167/iovs.09-3443
- [64] Liang F-Q, Green L, Wang C, Alssadi R, Godley BF. Melatonin protects human retinal pigment epithelial (RPE) cells against oxidative stress. *Experimental Eye Research*. 2004;**78**:1069-1075. DOI: 10.1016/j.exer.2004.02.003
- [65] Spinazzola A, Zeviani M. Disorders of nuclear-mitochondrial intergenomic

- signaling. *Gene*. 2005;**354**:162-168. DOI: 10.1016/j.gene.2005.03.025
- [66] SanGiovanni JP, Arking DE, Iyengar SK, Elashoff M, Clemons TE, Reed GF, et al. Mitochondrial DNA variants of respiratory complex I that uniquely characterize haplogroup T2 are associated with increased risk of age-related macular degeneration. *PLoS One*. 2009;**4**:e5508. DOI: 10.1371/journal.pone.0005508
- [67] Wang AL, Lukas TJ, Yuan M, Du N, Tso MO, Neufeld AH. Autophagy and exosomes in the aged retinal pigment epithelium: Possible relevance to drusen formation and age-related macular degeneration. *PLoS One*. 2009;**4**:e4160. DOI: 10.1371/journal.pone.0004160
- [68] Bakeeva LE, Skulachev VP, Sudarikova YV, Tsyplenkova VG. Mitochondria enter the nucleus (one further problem in chronic alcoholism). *Biochemistry Biokhimiia*. 2001;**66**:1335-1341. DOI: 10.1023/A:1013374410540
- [69] Delsite R, Kachhap S, Anbazhagan R, Gabrielson E, Singh KK. Nuclear genes involved in mitochondria-to-nucleus communication in breast cancer cells. *Molecular Cancer*. 2002;**1**:6. Available from: <http://www.pubmedcentral.nih.gov/articlerender.fcgi?artid=149409&tool=pmcentrez&rendertype=abstract>
- [70] Amuthan G, Biswas G, Zhang SY, Klein-Szanto A, Vijayasathya C, Avadhani NG. Mitochondria-to-nucleus stress signaling induces phenotypic changes, tumor progression and cell invasion. *The EMBO Journal*. 2001;**20**:1910-1920. DOI: 10.1093/emboj/20.8.1910
- [71] Park SY, Lee S, Park KS, Lee HK, Lee W. Proteomic analysis of cellular change involved in mitochondria-to-nucleus communication in L6 GLUT4myc myocytes. *Proteomics*. 2006;**6**:1210-1222. DOI: 10.1002/pmic.200500284
- [72] Woo DK, Phang TL, Trawick JD, Poyton RO. Multiple pathways of mitochondrial-nuclear communication in yeast: Intergenomic signaling involves ABF1 and affects a different set of genes than retrograde regulation. *Biochimica et Biophysica Acta*. 2009;**1789**:135-145. DOI: 10.1016/j.bbagr.2008.09.008
- [73] Yakes FM, Van Houten B. Mitochondrial DNA damage is more extensive and persists longer than nuclear DNA damage in human cells following oxidative stress. *Proceedings of the National Academy of Sciences of the United States of America*. 1997;**94**:514-519. DOI: 10.1073/pnas.94.2.514
- [74] Blasiak J, Glowacki S, Kauppinen A, Kaarniranta K. Mitochondrial and nuclear DNA damage and repair in age-related macular degeneration. *International Journal of Molecular Sciences*. 2013;**14**:2996-3010. DOI: 10.3390/ijms14022996
- [75] Abu-Asab MS, Salazar J, Tuo J, Chan C-C. Systems biology profiling of AMD on the basis of gene expression. *Journal of Ophthalmology*. 2013;**2013**:453934. DOI: 10.1155/2013/453934
- [76] Sreekumar PG, Ishikawa K, Spee C, Mehta HH, Wan J, Yen K, et al. The mitochondrial-derived peptide humanin protects RPE cells from oxidative stress, senescence, and mitochondrial dysfunction. *Investigative Ophthalmology & Visual Science*. 2016;**57**:1238-1253. DOI: 10.1167/iovs.15-17053
- [77] Biasutto L, Chiechi A, Couch R, Liotta VE. Retinal pigment epithelium (RPE) exosomes contain signaling phosphoproteins affected by oxidative stress. *Experimental Cell Research*. 2013;**319**:2113-2123. DOI: 10.1016/j.yexcr.2013.05.005